Joining phenomena and tensile strength of friction welded joint between pure titanium and low carbon steel

Masaaki Kimura[a,*], Tsukasa Iijima[b], Masahiro Kusaka[a], Koichi Kaizu[a] and Akiyoshi Fuji[c]

a* Department of Mechanical and System Engineering, Graduate School of Engineering, University of Hyogo, 2167 Shosha, Himeji, Hyogo 671-2280, Japan.

b Graduate student, University of Hyogo, 2167 Shosha, Himeji, Hyogo 671-2280, Japan

c Department of Mechanical Engineering, National University Corporation-Kitami Institute of Technology, 165 Koen-cho, Kitami, Hokkaido, 090-8507, Japan

This paper describes the effect of the friction welding condition on the joining phenomena and the tensile strength of friction welded joint between pure titanium (P-Ti) and low carbon steel (LCS). The adjacent region of the weld interface at the P-Ti side was intensely upsetting with accompanied large deformation of itself when the joint had sparkle at both applied friction pressures of 30 and 90 MPa, although that of the LCS side was hardly upset. The temperature of the whole weld interface at a friction pressure of 30 MPa reached to 1,150 K or over at a friction time of 3.0 s or longer. However, the half radius and centreline portion temperatures of the weld interface at a friction pressure of 90 MPa was not reached to 1,150 K, although the periphery portion of that was reached to its temperature. The central portion of the weld interface at a friction pressure of 90 MPa was deformed to a convex shape from the viewpoint of the P-Ti side, although that of 30 MPa remained almost flat after when the friction torque reached the initial peak. When the joint was made at a friction pressure of 30 MPa, a friction time of 3.0 s or longer, and a forge pressure of 270 MPa or higher, it achieved 100% joint efficiency and the P-Ti base metal fracture with no crack at the weld interface. However, many joints at friction times of 1.2 and 1.5 s fractured at the weld interface, although those achieved 100% joint efficiency, because whole weld interface temperature was below 1,150 K. On the other hand, many joints at a friction pressure of 90 MPa with high forge pressure also fractured at the weld interface, although those achieved 100% joint efficiency, because the weld interface temperature at the half radius and periphery portions was below 1,150 K. Those joints did not have the intermetallic compound layer at the weld interface. The difference of the fractured portion of the joint in both applied friction pressures was due to the difference between the maximum temperature at the weld interface during the friction process and the deformation amount of the LCS side caused by applied forge pressure. To obtain 100% joint efficiency with the P-Ti base metal fracture with no crack at the weld interface, the joint should be made with high forge pressure, low friction pressure, and with opportune friction time at which the temperature at whole weld interface reached around 1,150 K.

Keywords: Welding, Plastic behaviour, Non-ferros metals and alloys, Mechanical

1. Introduction

Titanium (Ti) and its alloys (referred to as Ti-system material) are well-known materials with highly attractive characteristics in terms of mechanical and metallurgical properties, e.g., high specific strength and excellent corrosion resistance. They are very widely used for the important structural components in aerospace vehicles, architecture, automobiles, and so on. Moreover, they are also useful as biomedical materials due to their low allergenic effect on the human body. On the other hand, fusion welding between Ti-system material and such other materials as steel, stainless steel, aluminium (Al), and copper (Cu) have poor mechanical properties due to the brittle intermetallic compound (IMC) layer produced at the joint interface [1,2]. Therefore, a welding process for between Ti-system material and other material joints which will result in less degradation of the mechanical and metallurgical properties of the joint is urgently required.

The solid state joining methods such as diffusion welding, friction welding, and friction stir welding, can be applied to join between Ti-system material and other materials. Some researchers have reported that the mechanical and metallurgical properties of the friction welded joints of Ti-system materials and various steels [3-5] or stainless steels [6-12] show desirable characteristics. For example, the friction welding condition for the joint which had the good tensile strength of pure Ti and stainless steel joint was individually demonstrated as following combinations: pure Ti and American Iron and Steel Institute (AISI) standard type 321 stainless steel of Lee et al. [6], pure Ti and AISI 304L stainless steel of Dey et al. [7], and pure Ti and AISI 316 stainless steel of Akbarimousavi et al. [8]. In addition, Fuji et al. [9-11] showed the results of the good tensile strength and bend ductility and improving point of those mechanical properties for pure Ti and AISI 304L stainless steel joint. Ochi et al. [12] also showed the results of X-ray diffraction analysis at the fractured surface of pure Ti and AISI 304 stainless steel joint. In those ways, some researchers have reported that the joining of Ti-system materials and stainless steels could be successfully achieved and a relatively good joint was obtained. On the other hand, research on the friction welding of the combination between Ti-system materials and various steels has been slight in comparison with that of Ti-system materials and stainless steels, because the friction weldability of the former combination differed with the latter combination [13]. In this case, the friction welding condition for the joint which had the good tensile strength of pure Ti and steel joint was individually showed: the combination between pure Ti and plain carbon steel of Hasui et al. [3] and pure Ti and the combination between medium carbon steel of Shinoda et al. [4]. Also, Meshram et al. [5] showed the results of SEM-EPMA analysis at the adjacent region of the weld interface for the joint of combination between Ti and Fe. However, the joining mechanism of dissimilar materials friction welding between Ti-system materials and various steels has not been fully clarified, so that the friction welding conditions for material combinations are determined by trial and error. That is, the joining mechanism of friction welding for dissimilar materials was not clarified, and the condition that the joint does not fracture at the weld interface when it will be satisfied with some state was not theoretically displayed. Furthermore, the joining mechanism of friction welding of dissimilar materials differs from that of similar materials, because mechanical properties such as the tensile strength and thermal properties such as the thermal conductivity are different in their combinations. To determine the friction welding conditions theoretically, it is very essential to clarify the joining phenomena and the joint mechanical properties. In particular, clarifications of the joining mechanism are strongly required concerning the weldability between the Ti-system materials and other material such as steel, because an expansion in the use of Ti-system material and steel is expected and widely used in various component parts.

In previous works [14-20], the authors clarified the joining mechanism during the friction welding process of similar material combinations which were various carbon steels or Al-system materials. Furthermore, the authors also clarified the joining mechanism during the friction welding process of some dissimilar material joints as following combinations: Al-system materials and pure Cu [21], Al-system materials and low carbon steel [22,23], Cu-system materials and low carbon steel [24,25], and pure Cu and pure Ti [21,26]. If combinations of dissimilar materials such as Ti-system materials and steel can be joined using the same method as that shown in previous reports [14-26], the joining mechanism will be clarified. In particular, to clarify the effect of the friction pressure on joining phenomena of the Ti-system materials and steel joint is strongly important, because the joining phenomena between pure Ti and pure Cu were affected by the friction pressure, and the difference of that was the yield stress for each material depended on the temperature in the friction process [26].

Based on the above background, the authors have been carrying out research to clarify the joining mechanism between dissimilar materials in the friction process. The authors investigate the joining phenomena during the friction process of friction welds between pure Ti and low carbon steel in the present work. The authors also demonstrate the results of the joining phenomena at various friction pressures. In addition, the authors show the joint tensile properties under various friction welding conditions, i.e. the effect of friction pressure, friction time, and forge pressure on the joint tensile strengths is clarified. Furthermore, the authors show the friction welding conditions for a joint that had the same tensile strength as the pure Ti base metal and fractured on the pure Ti side with no crack at the weld interface.

2. Experimental procedure

The materials used were commercially pure Ti (referred to as P-Ti) and low carbon steel (referred to as LCS) in 16 mm diameter rods. Although the chemical composition of the P-Ti was 0.001H-0.089O-0.006N-0.005C-0.038Fe in mass%, two kinds of P-Ti having slightly different tensile properties were used for this experiment because they had different production lots. The ultimate tensile strengths of the P-Ti were 401 and 379 MPa, the 0.2% yield strengths were 304 and 301 MPa, and the elongations were 35 and 39%, respectively. On the other hand, the chemical composition of LCS was 0.16C-0.45Mn-0.20Si-0.12P-0.18S in mass%, its ultimate tensile strength was 448 MPa, its yield strength was 291 MPa, and its elongation was 35%. Those materials were machined to 12 mm in diameter of the weld faying (contacting) surface. In addition, the temperature changes during the friction process at the centreline, half radius, and periphery portions of the 1.0 mm longitudinal direction from the weld faying surface were measured using the LCS specimen. In this connection, the sufficient data could be obtained in order to understand the temperature distribution of the radius direction at the weld interface, although the weld interface temperature was able to estimate as this temperature or higher. The details of the specimen shape for measuring temperature changes have been described in previous reports [22-27]. All weld faying surfaces of the specimens were polished with a surface grinding machine before joining to eliminate the effect of surface roughness on the joining behaviour. In this case, the centreline average height of the roughness of the P-Ti side specimen was about 0.34 μm, and the LCS side specimen was about 0.10 μm.

A continuous (direct) drive friction welding machine was used for the joining. This friction welding machine had three kind of welding method as follows.

(1) The conventional friction welding method that have the braking system when the friction time expired, for measuring the friction torque and the temperature change at the weld interface.
(2) The welding method that the fixed side specimen is simultaneously and forcibly separated from the rotating side specimen when the friction time expired, for observation of the transitional changes

at the weld interface.

(3) The welding method that the relative speeds at the weld interface between both specimens simultaneously is decreased to zero when the friction time expired to prevent braking deformation during rotation stop, for observation of the cross-section at the weld interface region.

To clarify the joining phenomena during the friction process, the authors carried out three above welding methods. In particular, the experimental methods of (2) and (3) were used to obtain the joint without braking deformation. The details of these methods have been described in previous reports [14-26,28]. During friction welding operations, the friction speed and pressure were set to the following combinations: 27.5 s^{-1} (1650 rpm) for 30 MPa and 27.5 s^{-1} for 90 MPa. The forge pressure was applied at an identical friction pressure. The joining behavior was recorded by a digital video camera. The friction torque was measured with a load-cell, and the temperatures were measured with a mineral insulated thermocouple with a chromel-alumel. The friction torque and temperature were recorded with a personal computer through an A/D converter with a sampling time of 0.001 s. In addition, analysis via SEM-EDS was carried out to analyze the chemical composition in the weld interface region. On the other hand, all joint tensile test specimens were machined to 12 mm diameters and 66 mm in parallel length. That is, all flash (burr or collar), which was exhausted from the weld interface during the friction welding process, were removed from the joint for joint tensile test specimen. Then, the joint tensile test was carried out with as-welded condition at room temperature.

3. Results

3.1 Relationship between joining behaviour and friction torque

Figure 1 shows the relationship between the joining behaviour and the friction torque with a friction pressure of 30 MPa. Photos 1) to 6) in Fig. 1a correspond to the friction torque of (1) to (6) in Fig. 1b, respectively. Photo 1) shows the state at the weld faying surfaces as they contacted each other, then the friction torque was increased. The colour on the adjacent region of the weld

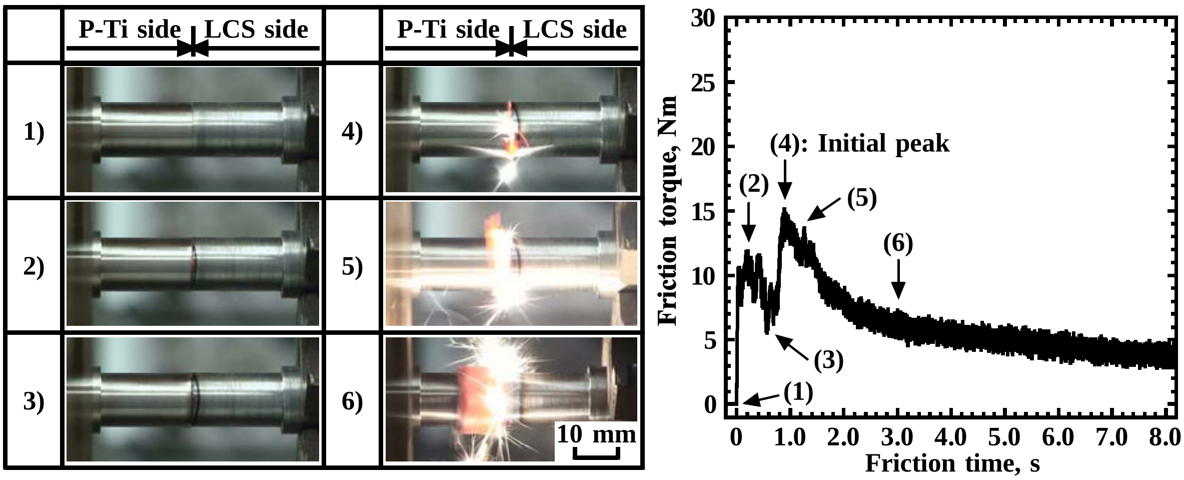

(a) Joining behaviour (b) Friction torque curve

Fig. 1 Joining behaviour and friction torque curve during friction process; friction pressure of 30 MPa.

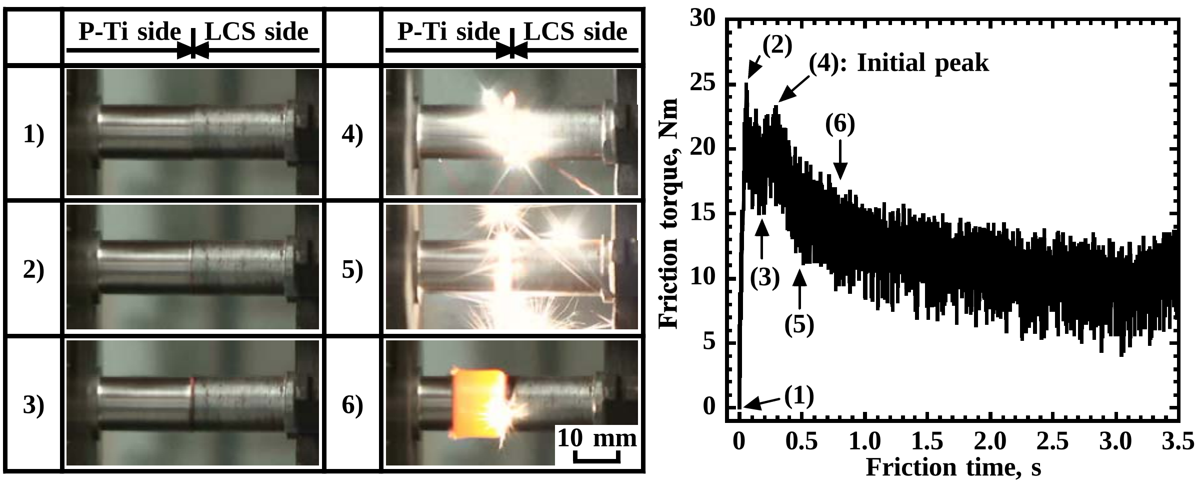

(a) Joining behaviour (b) Friction torque curve

Fig. 2 Joining behaviour and friction torque curve during friction process; friction pressure of 90 MPa.

interface at the LCS side outer surface was changed to blue as shown in photo 2) at the friction torque of (2). Then, when the friction torque decreased to (3), the adjacent region of the weld interface at the P-Ti side was slightly upsetting with accompanied deformation of itself as shown in photo 3). Immediately after that behaviour, the P-Ti side was sparkled from the weld interface as shown in Photo 4) when the friction torque reached the initial peak of (4). The initial peak torque was approximately 15 Nm, and the elapsed time for the initial peak was about 0.9 s. Thereafter, the friction torque decreased with increasing friction time between (5) and (6). Also, the sparkle kept generating from the weld interface after the initial peak, and the upsetting and the flash of P-Ti increased with increasing friction time although the LCS side was not upset, as shown in photos 5) and 6).

Figure 2 shows the relationship between the joining behaviour and the friction torque with a friction pressure of 90 MPa. Photos 1) to 6) in Fig. 2a correspond to friction torques (1) to (6) in Fig. 2b. Photo 1) shows when the weld faying surfaces initially contacted each other. Photo 2) was similar to 1), although the friction torque increased to (2). Then, when the friction torque decreased to (3), the P-Ti side was slightly upset as shown in photo 3). Immediately after that behaviour, the P-Ti side was sparkled from the weld interface as shown in Photo 4) at the friction torque reached the initial peak of (4). This initial peak torque was approximately 23 Nm, and the elapsed time for this initial peak was about 0.3 s. This initial peak torque was higher than that of 30 MPa, and this elapsed time for the initial peak was shorter than that of 30 MPa. Thereafter, the friction torque decreased and the upsetting and the flash of P-Ti increased with increasing friction time, as shown in photos 5) and 6). However, the LCS side was hardly upset as shown in photos 5) and 6) although the sparkle also kept generating from the weld interface. Therefore, the joining behaviour during the friction process under a friction pressure of 90 MPa resembled that of 30 MPa, although the friction torque curves were different. This result differed with the joining behaviour of the friction welding under the same friction pressure between P-Ti and pure Cu [26].

3.2 Temperature change during friction process

Figures 3 and 4 show the temperature changes with the friction torques during the friction process with friction pressures of 30 and 90 MPa, respectively. When the friction pressure was 30 MPa as shown in Fig. 3, the temperatures at the centreline, half radius and periphery portions of the weld interface at the LCS side were almost the same. The temperatures of all measured portions were increased with increasing friction time, and then those were reached to approximately 950 K at a friction time of about 1.2 s, i.e. the friction torque reached after the initial peak. Then, those temperatures increased with increasing friction time and reached to approximately 1,150 K at a friction time of about 3.0 s. This temperature was close to the temperature of the P-Ti base metal which intensely reacts with O_2 or N_2, although that will be described later [29,30]. Then, the gradient of those temperatures changed gradually rise about this friction time, and those were maintained nearly constant at a friction time of 3.0 s or longer. The temperatures of all measured portions were approximately 1,200 K at a friction time of 8.0 s. On the other hand, although all measured temperatures were almost the same before a friction time of 0.7 s, the temperature at after this friction time was high in order of the periphery, half radius, and centreline portions, when the joint was made at a friction pressure of 90 MPa as shown in Fig. 4. The difference in each temperature was approximately 50 K at a friction time of 1.5 s or longer. In addition, the maximum temperatures with a friction pressure of 90 MPa were lower than those of 30 MPa, although the friction torque varied. This result was due to the change of the yield

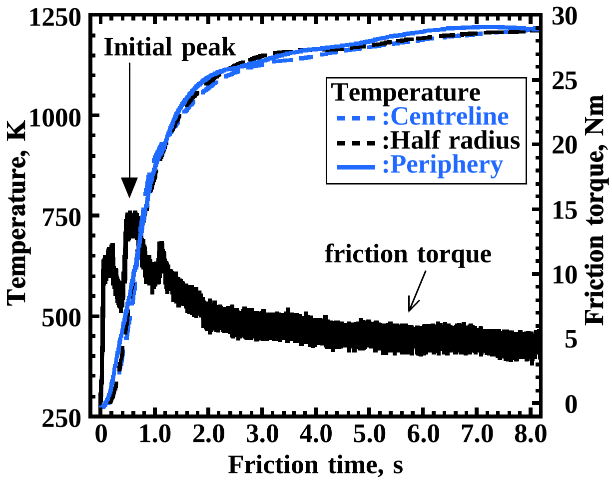

Fig. 3 Relationship between friction time and temperature changes at various measured portions of LCS side during friction process, in relation to friction torque curve; friction pressure of 30 MPa.

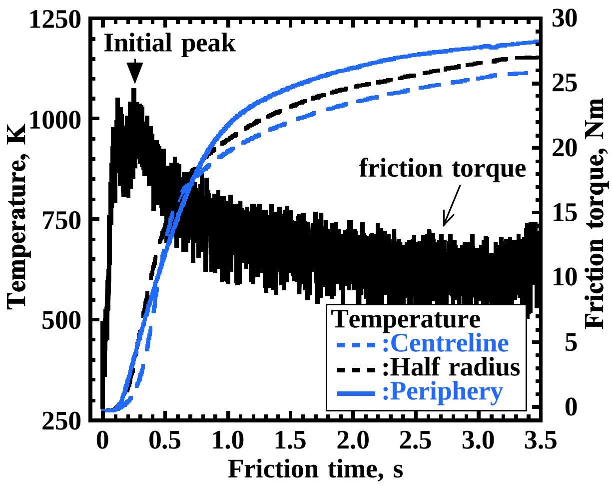

Fig. 4 Relationship between friction time and temperature changes at various measured portions of LCS side during friction process, in relation to friction torque curve; friction pressure of 90 MPa.

stress of the P-Ti base metal with the temperature. That is, the temperature of the high strength was lower than that of the low strength, when the P-Ti base metal is deformed under applied friction pressure. These details will be described later. Furthermore, this difference in the measured temperatures under both friction pressures resembled that of some dissimilar friction welded joints at the same friction pressures [24-26].

3.3 Transitional changes of weld interface

Figure 5 shows the examples of the appearances of the weld interfaces after welding at various friction times with a friction pressure of 30 MPa. When the

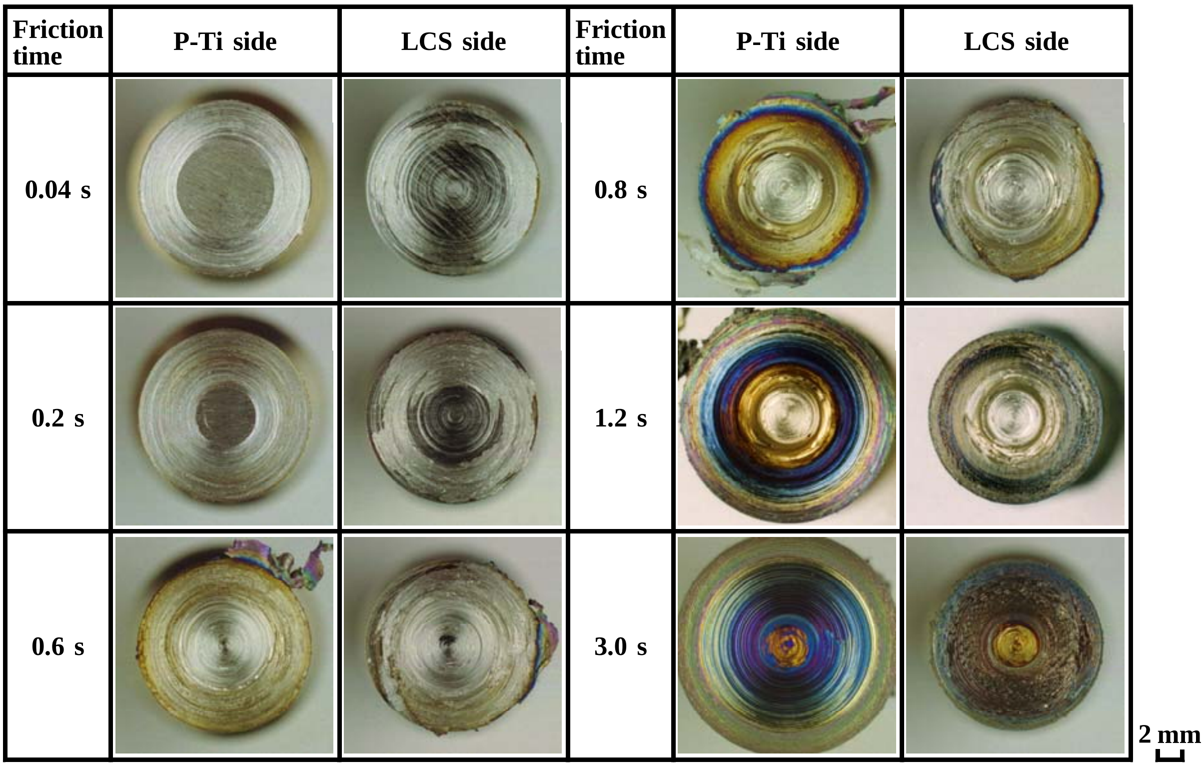

Fig. 5 Appearances of weld interfaces after welding at various friction times; friction pressure of 30 MPa.

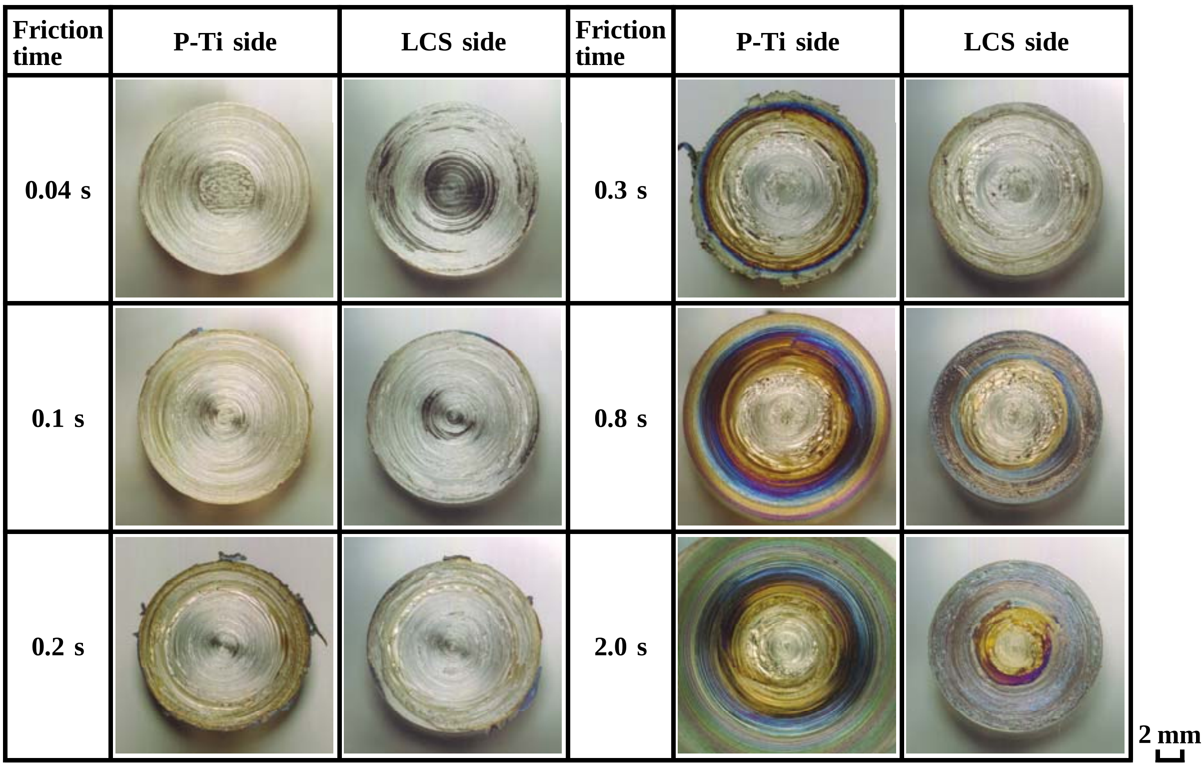

Fig. 6 Appearances of weld interfaces after welding at various friction times; friction pressure of 90 MPa.

friction time was 0.04 s, i.e. both specimens had been rotated once, the concentric rubbing marks were observed at the half radius and peripheral regions in the weld interface of both sides. Also, the weld interface at the LCS side was slightly roughened, i.e. it was the P-Ti which transferred to the LCS side from the P-Ti side. The concentric rubbing marks in both weld interfaces and the transferred P-Ti on the LCS side extended to the central region with increasing friction time as shown at a friction time of 0.2 s. When the friction time was 0.6 s, the P-Ti flash was exhausted to the radial direction of the weld interface, and the colour at the peripheral region of the P-Ti side turned to primrose yellow. The transferred P-Ti on the LCS side also increased. When the friction time was 0.8 s, i.e. the friction torque close to the initial peak, the exhausted flash of the P-Ti increased and the colour of the peripheral region at the P-Ti side turned to blue. However, the central region of both weld interfaces did not have the concentric rubbing marks at this friction time. When the friction time was 1.2 s, the entire weld interface had the concentric rubbing marks, and the blue colour area of the P-Ti side extended to its central region. In addition, the peripheral region at the LCS side became colourful. Then, almost whole weld interface at the P-Ti side turned to blue, and it became slightly flat at a friction time of 3.0 s. Also, the whole LCS side became colourful. Both weld interfaces at long friction time resembled that of 3.0 s, in spite of the quantity of the P-Ti flash differed (data not shown due to space limitations). However, the LCS flash was hardly observed at all friction times.

Figure 6 shows the examples of the appearances of the weld interfaces after welding at various friction times with a friction pressure of 90 MPa. When the friction time was 0.04 s, the concentric rubbing marks were observed at almost whole weld interface without the central region of both sides. Also, the P-Ti transferred was observed at those regions on the LCS side. The concentric rubbing marks and the transferred P-Ti extended to the central region of both sides with increasing friction time. In addition, the colour at the peripheral region of the P-Ti side turned to primrose yellow as shown at a friction time of 0.1 s. When the friction time was 0.2 s, the P-Ti flash was exhausted although the central region of both sides did not have the concentric rubbing marks. Then, the entire weld interface of both sides had the concentric rubbing marks when the friction time was 0.3 s, i.e. the friction torque just reached the initial peak. Furthermore, the P-Ti flash increased and the peripheral region of the P-Ti side turned to blue. Thereafter, the P-Ti flash increased with increasing friction time, and both weld interfaces became colourful, in spite of the quantity of the P-Ti flash differed. The peripheral region of the P-Ti side became slightly flat although the central region of it was rough. According to these results, the entire weld interface had transferred P-Ti on the LCS side when the friction torque reached the initial peak at these friction pressures, and then the P-Ti side flash increased with increasing friction time.

3.4 Observation of cross-section of weld interface region

Figure 7 shows the cross-sectional appearances of the weld interface regions of the joints at various at various friction times with a friction pressure of 30 MPa. When the joint was made at a friction time of 0.6 s as shown in Fig. 7a, the weld interface was clear and almost flat. However, this joint had such defects as a not-joined region at the peripheral portion of the weld interface indicated by oval lines in this picture, although the P-Ti was slightly exhausted as flash from the peripheral portion. The P-Ti flash was increased with increasing friction time, and then the not-joined region was not observed at the weld interface when the friction time was 1.0 s, i.e. the friction torque reached the initial peak (Fig. 7b). That is, it was considered that the P-Ti side and LCS side were completely joined at this friction time. Thereafter, the weld interface remained almost flat, and the LCS side was not deformed with increasing friction time, although the quantity of the flash at P-Ti

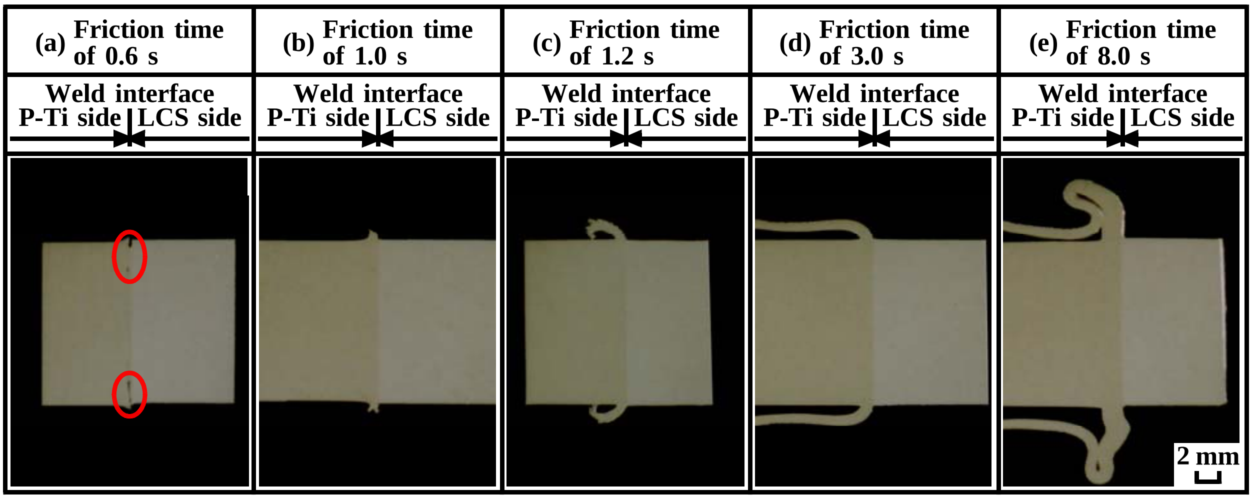

Fig. 7 Cross-sectional appearances of weld interface region of joints at various friction times; friction pressure of 30 MPa.

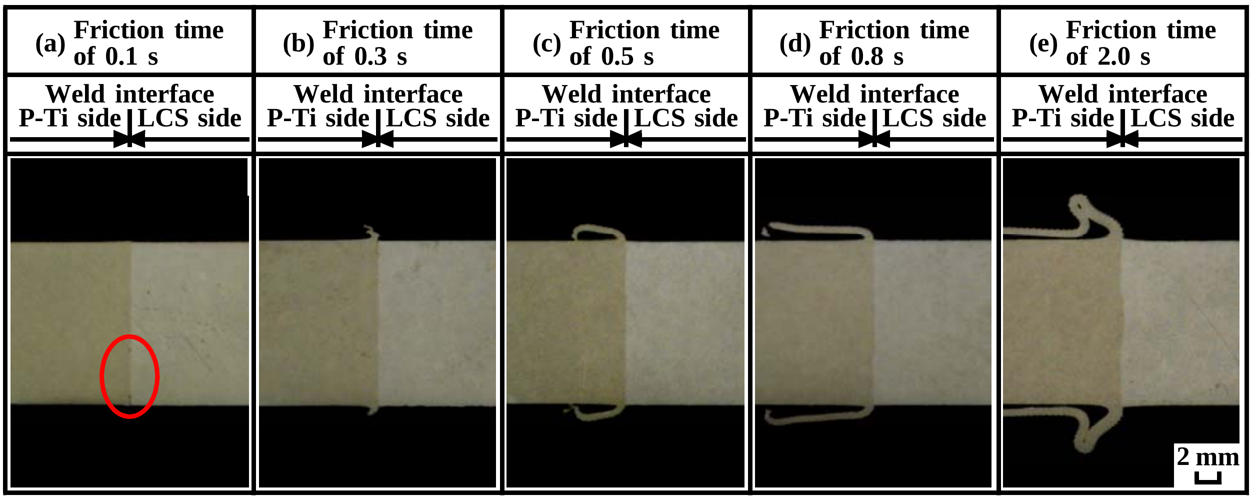

Fig. 8 Cross-sectional appearances of weld interface region of joints at various friction times; friction pressure of 90 MPa.

increased (Figs. 7c through 7e). In addition, the weld interface did not have a not-joined region after the friction time when the friction torque reached the initial peak.

Figure 8 shows the cross-sectional appearances of the weld interface region of the joint at various friction times with a friction pressure of 90 MPa. The joint at a friction time of 0.1 s as shown in Fig. 8a had a not-joined region at the peripheral portion that indicated by an oval line in this picture, although the weld interface was clear and almost flat. Also, the P-Ti flash was slightly exhausted. When the friction time was 0.3 s, i.e. the friction torque reached the initial peak, the weld interface was completely joined and the P-Ti flash increased (Fig. 8b). The P-Ti flash increased and the weld interface remained almost flat with increasing friction time as shown in the joint at a friction time of 0.5 s as shown in Fig. 8c. Then, the central portion at the P-Ti side was slightly deformed to a convex shape from the viewpoint of the P-Ti side, i.e. the weld interface was not flat, which was indicated as the joint of a friction time of 0.8 s (Fig. 8d). Thereafter, the P-Ti side remained a convex shape as shown in the joint at a friction time of 2.0 s (Fig. 8e). However, the LCS flash was hardly exhausted although the quantity of P-Ti flash increased. The fact that the weld interface shape had dissimilarity was due to the difference of the temperature at the weld interface with applied friction pressure (see Figs. 3 and 4).

3.5 SEM observation and EDS analysis of weld interface region

Figures 9 and 10 show the SEM image and EDS analysis result at the periphery portion of the weld interface region of the joint. In this case, the joint for Fig. 9 was made with a friction pressure of 30 MPa, a friction time of 3.0 s, and a forge pressure of 30 MPa. Also, the joint for Fig. 10 was made with a friction pressure of 90 MPa, a friction time of 2.0 s, and a forge pressure of 90 MPa. When the joint was made at a friction pressure of 30 MPa as shown in Fig. 9, the distribution lines corresponding to Ti and Fe by EDS analysis had no plateau part at the weld interface although the weld interface was slightly unclear. Moreover, when the joint was made at a friction pressure of 90 MPa as shown in Fig. 10, the weld interface was relatively clear, and the distribution lines corresponding to Ti and Fe had also no plateau part at the weld interface. The joints with other friction times

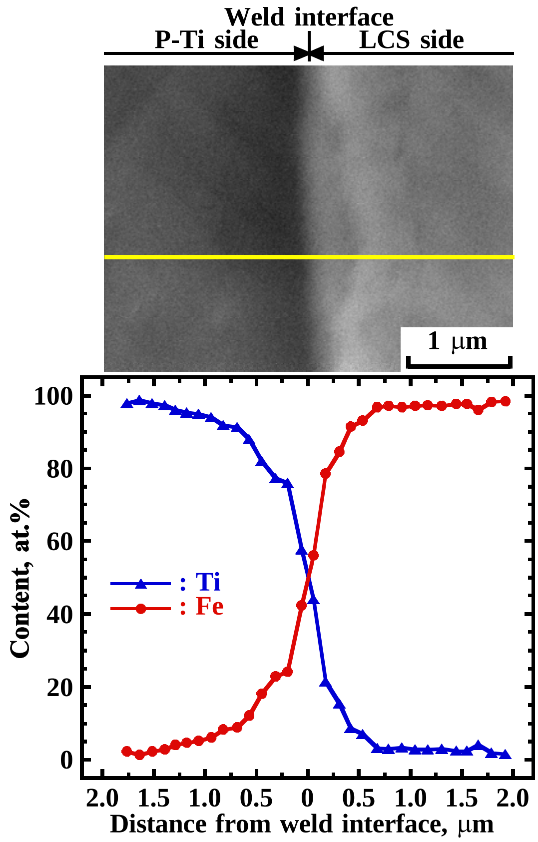

Fig. 9 SEM image and EDS analysis result at periphery portion of weld interface region; friction pressure of 30 MPa, friction time of 3.0 s, and forge pressure of 30 MPa.

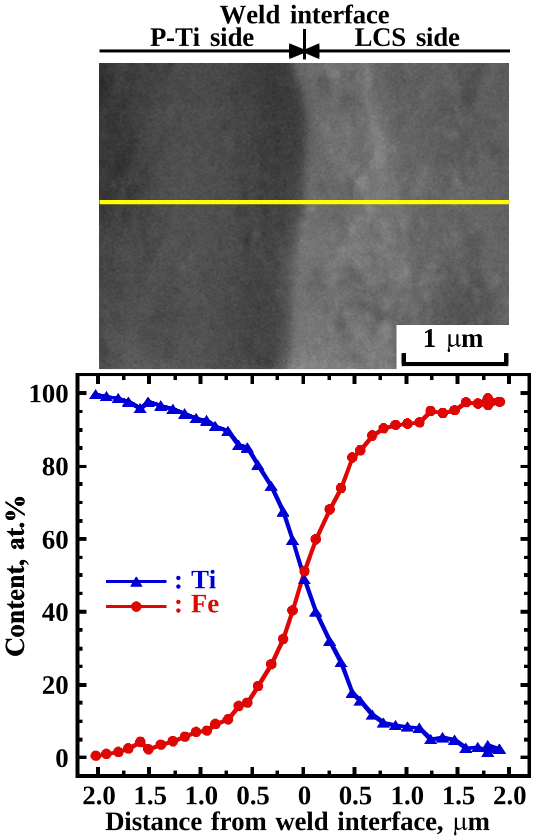

Fig. 10 SEM image and EDS analysis result at periphery portion of weld interface region; friction pressure of 90 MPa, friction time of 2.0 s, and forge pressure of 90 MPa.

as well as the other portions of these joints also did not have the IMC layer, although the temperature of the radius direction in the weld interface or the maximum temperature at the weld interface caused by the applied friction pressure differed as shown in Figs. 3 and 4. Therefore, an IMC layer was not observed at the weld interface with applied friction pressures of 30 and 90 MPa, which was based on the SEM observation level.

3.6 Relationship between joint tensile strength and friction time

Figure 11 shows the relationship between the friction time and the joint efficiency of the joint, plotted alongside the friction torque curve at a friction pressure of 30 MPa. The joint efficiency was defined as the ratio of joint tensile strength to the ultimate tensile strength of the P-Ti base metal. Figure 12 shows the example of the appearance of the joint tensile test specimen with the weld interface fracture after tensile testing. In this case, forge pressure was applied at an identical friction pressure, i.e. 30 MPa. The joint efficiency at a friction time of 0.5 s was approximately 6% and it had a scattering. The joint fractured at the weld interface as shown in Fig. 12, although it had a little P-Ti adhering on the LCS side interface. In this connection, the P-Ti and LCS were not welded before a friction time of 0.5 s because a sufficient quantity of friction heat for welding

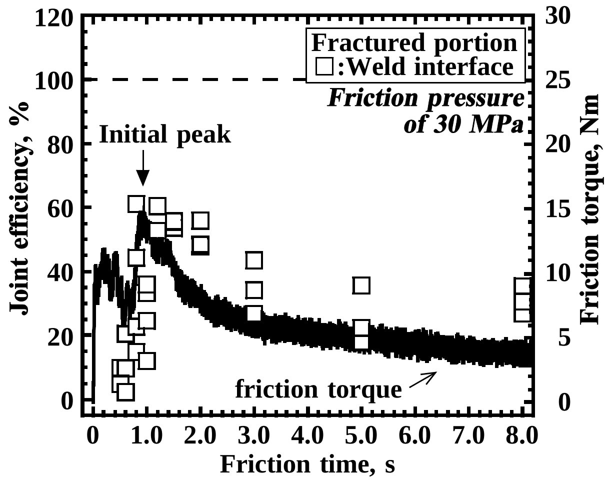

Fig. 11 Relationship between friction time and joint efficiency of joint, in relation to friction torque; friction pressure of 30 MPa and forge pressure of 30 MPa.

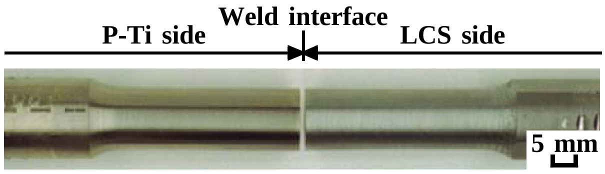

Fig. 12 Example of appearance of joint tensile test specimen with weld interface fracture after tensile testing.

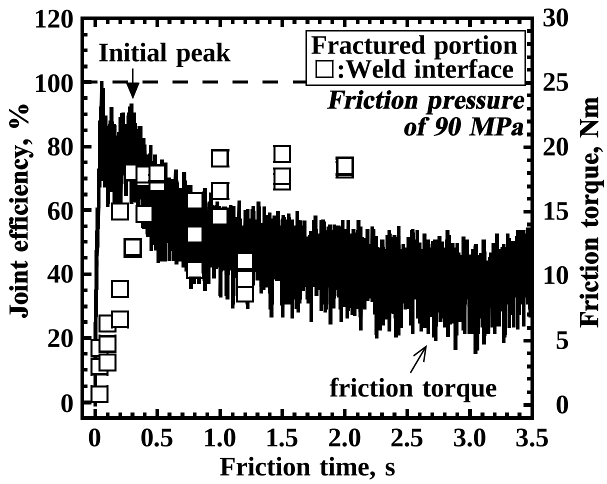

Fig. 13 Relationship between friction time and joint efficiency of joint, in relation to friction torque; friction pressure of 90 MPa and forge pressure of 90 MPa.

could not be produced. The joint efficiency increased with increasing friction time, and then the joint had approximately 55% efficiency at a friction time of 1.2 s, i.e. the friction torque reached just after the initial peak. However, the joint efficiency decreased to approximately 35% at a friction time of 3.0 s, and it had almost same joint efficiency at a friction time of 8.0 s. That is, the joint at a friction pressure of 30 MPa did not achieve 100% joint efficiency and it was fractured at the weld interface at all friction times as shown in Fig. 12.

Figure 13 shows the relationship between the friction time and the joint efficiency of the joint, plotted alongside the friction torque curve at a friction pressure of 90 MPa. In this case, forge pressure was applied at an identical friction pressure, i.e. 90 MPa. The joint efficiency at a friction time of 0.1 s was approximately 18%, and the joint had the weld interface fracture as shown in Fig. 12. The joint efficiency increased with increasing friction time, and it was approximately 56% at a friction time of 0.3 s, i.e. the friction torque reached just the initial peak. Thereafter, the joint efficiency was kept with scattered measurements from 30 to 75% after this friction time. That is, although the joint efficiency was higher than that of 30 MPa, the joint at a friction pressure of 90 MPa also did not achieve 100% efficiency and it was fractured at the weld interface at all friction times as shown in Fig. 12. Furthermore, the weld interface did not have the IMC layer at all fractured surfaces, as shown in Figs. 9 and 10. Therefore, it was clarified that the joint did not achieve 100% efficiency due to not the generation of IMC at the weld interface but the poor strength between the P-Ti side and the LCS. Hence, the joint should be made with applying forge pressure that was higher than applied friction pressure.

4. Discussion

4.1 Consideration of joining phenomena by friction pressure

Based on the above results, the joining phenomena during the friction process of friction welding between P-Ti and LCS was similar although applied friction pressures are different. In brief, the P-Ti side was intensely upset while accompanied with sparkle after when the friction torque reached the initial peak. However, the LCS side hardly upset as shown in Figs. 1, 2, 7 and 8, although the yield strength of the P-Ti base metal was higher than that of the LCS base metal which described in the experimental procedure section. On the other hand, the joining phenomena of friction welding between P-Ti and pure Cu had significantly differed by applied friction pressure [26] although the joints between pure Cu or Brass and LCS had similar joining phenomena under different applied friction pressures [24,25]. That is, in the friction welding between pure Cu or Brass and LCS, pure Cu or Brass side was intensely upset although the LCS side hardly upset regardless of applied friction pressure [24,25]. In contrast of those phenomena, the upset side of the friction welding between P-Ti and pure Cu was changed by applied friction pressure [26]. Hence, it was able to be considered that the joining phenomena of friction welding between P-Ti and other materials differ with applied friction pressure. Moreover, the fact of the friction welding between P-Ti and pure Cu that the difference of the yield stress for each material depended on the temperature in the friction process because the yield stress of those materials were interchanged by the

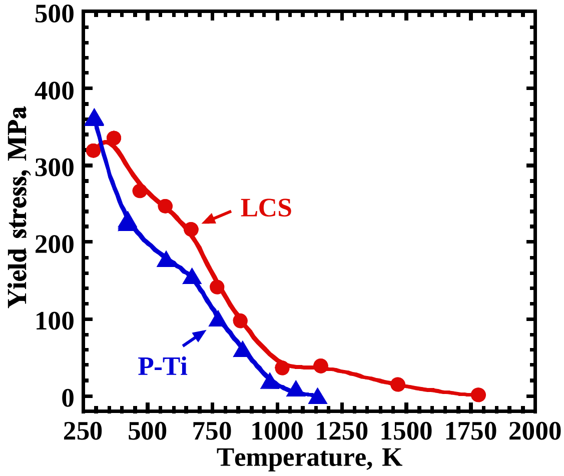

Fig. 14 Relationships between temperature and yield stress of pure Ti (P-Ti) and low carbon steel (LCS) base metals [15,21].

friction pressure was clarified in a previous report [26]. To clarify the joining phenomena of friction welding between P-Ti and LCS, the comparison of the yield stress of those materials is necessary. Figure 14 shows an excerpt from previous reports [15,21] of the relationships between temperature and the yield stress of P-Ti and LCS base metals. In this case, the ultimate tensile strength of P-Ti and LCS base metals was 397 and 445 MPa, and the 0.2% yield strength of those was 362 and 318 MPa, respectively, namely the used materials of this figure were differed from the specimens of friction welding in this report. In addition, the tensile test was carried out with a crosshead speed of 0.5 mm/min in the atmosphere environment, and the yield stress of P-Ti at a temperature of 1,158 K was plotted as zero, since the P-Ti base metal intensely reacted with O_2 or N_2 under the high temperature condition [29,30]. The details of the experimental method have been described in previous reports [15,21]. Excepting room temperature, the yield stress of P-Ti was lower than that of LCS, which was shown in Fig. 14. In case of the friction welding, it was able to be considered that the flash was exhausted from the weld interface of the joint during the friction process when the yield stresses of the base materials with temperature raise by the friction were less than applied friction pressure [15,17,21]. Hence, it was able to estimate that P-Ti was easily and consistently upset during the friction process from Fig. 14. Moreover, the fact that the weld interface at a friction pressure of 90 MPa was deformed to a convex shape from the viewpoint of the P-Ti side (Fig. 8), although that of 30 MPa remained almost flat (Fig. 7), was due to the difference of the maximum temperature at the weld interface with applied friction pressure (Figs. 3 and 4). That is, it was able to estimate from Fig. 4 that the temperature at the centreline portion in the weld interface after the initial peak with a friction pressure of 90 MPa was lower than that of the periphery portion. Therefore, the central portion at the P-Ti side was deformed to a convex shape

(Fig. 8) because the quantity of the exhausted flash at the peripheral portion of the weld interface at a friction pressure of 90 MPa was larger than that of the central portion. Furthermore, the weld interface at a friction pressure of 30 MPa remained almost flat (Fig. 7) because the temperature distribution of the radius direction at the weld interface seemed to be same (see Fig. 3).

Hence, it was clarified that the joining phenomena during the friction process at a friction pressure of 30 MPa were similar to that of 90 MPa, although the maximum temperature at the weld interface and the deformation of it differed. Incidentally, to make joints between Ti or its alloys and other materials should be necessary to note, because that may be generating sparkle from the weld interface of the Ti side by the combination of the materials (e.g., Figs. 1 and 2).

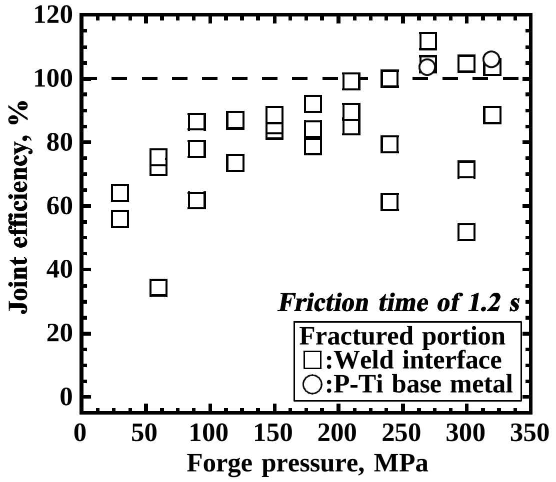

(a) Friction time of 1.2 s

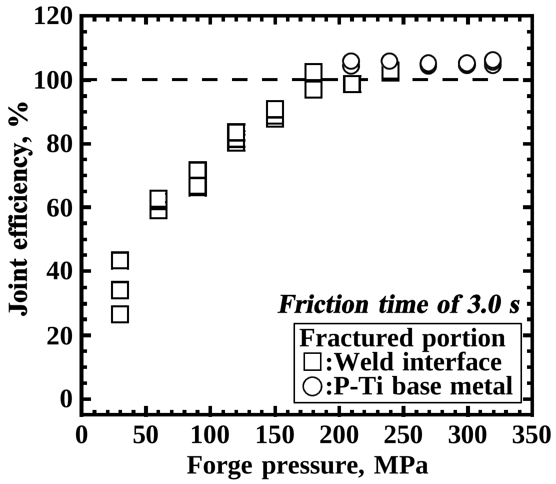

(b) Friction time of 3.0 s

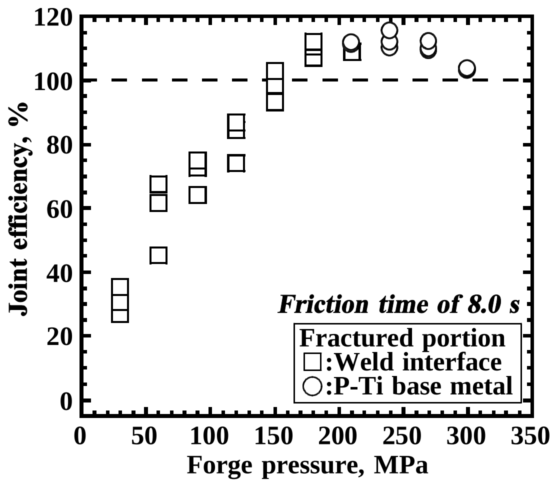

(c) Friction time of 8.0 s

Fig. 15 Relationship between forge pressure and joint efficiency of joint at various friction times; friction pressure of 30 MPa.

4.2 Improving joint efficiency

To improve the joint efficiency, the effect of forge pressure on joint efficiency was investigated. Figure 15 shows the relationship between the forge pressure and joint efficiency of the joints with a friction pressure of 30 MPa which were made at friction times of 1.2, 3.0 and 8.0 s. Figure 16 shows the appearance of the joint tensile test specimen with the P-Ti side fracture after tensile testing. The joint efficiency of the joint at a friction time of 1.2 s as shown in Fig. 15a, which the friction torque reached just after the initial peak, increased with increasing forge pressure although it had a scattering. Then, when the joint was made with a forge pressure of 270 MPa or higher, some joints had the same tensile strength as that of the P-Ti base metal. However, the joint efficiency had a scattering, and almost all joints fractured at the weld interface as shown in Fig. 12 although some joints had the P-Ti base metal fracture as shown in Fig. 16. That is, the joint, which had 100% joint efficiency with the P-Ti base metal fracture, was not easily obtained at a friction time of 1.2 s, because the weld interface temperature was able to estimate low (approximately 950 K) at this friction time (see Fig. 3). The details will be described later. In this

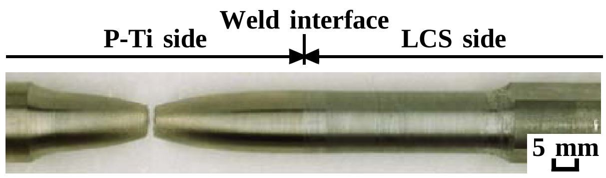

Fig. 16 Example of appearance of joint tensile test specimen with P-Ti base metal fracture after tensile testing.

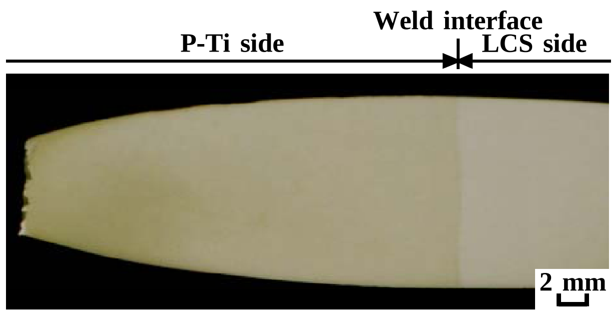

Fig. 17 Example of cross-sectional appearance of fractured specimen with P-Ti base metal fracture of joints after tensile testing.

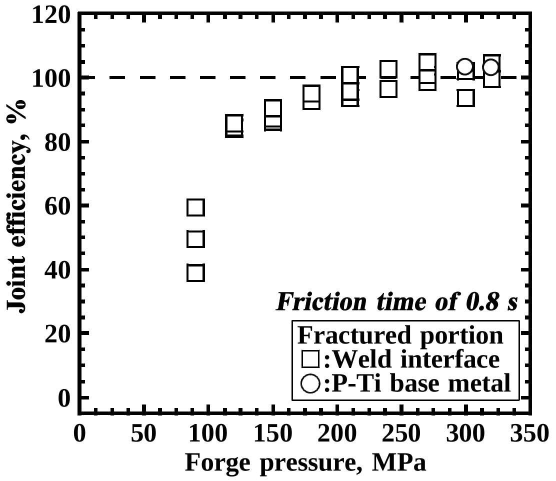

(a) Friction time of 0.8 s

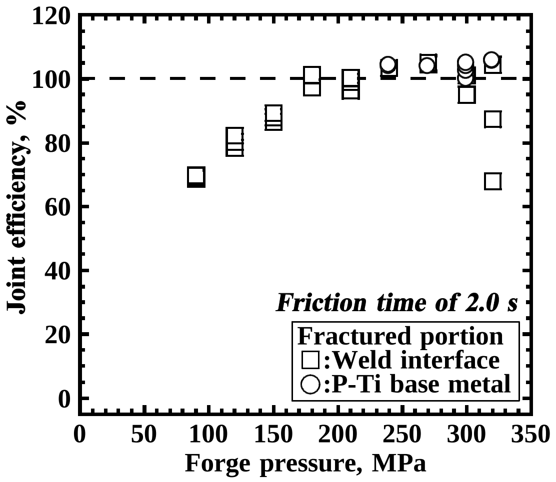

(b) Friction time of 2.0 s

Fig. 18 Relationship between forge pressure and joint efficiency of joint at various friction times; friction pressure of 90 MPa.

case, the joint efficiency of some joints was obtained 100% or higher because the parallel part length of the joint tensile specimen was shorter. On the other hand, the joint efficiency of the joint at a friction time of 3.0 s, which the temperature at whole weld interface achieved approximately 1,150 K (see Fig. 3), also increased with increasing forge pressure, as shown in Fig. 15b; incidentally, this temperature was close to the temperature of the P-Ti base metal which intensely reacts with O_2 or N_2 [29,30]. In addition, the scattering of the joint efficiency decreased. The joint efficiency achieved 100% at a forge pressure of 210 MPa, and then all joints fractured from the P-Ti base metal as shown in Fig. 16 when the joint was made with a forge pressure of 270 MPa or higher. Figure 17 shows the cross-sectional appearance of the joint tensile test specimen with the P-Ti base metal fracture after tensile testing. The weld interface of the joint had neither a not-joined region nor a defect after tensile testing. That is, P-Ti and the LCS were tightly joined. Moreover, the joint efficiency at a friction time of 8.0 s as shown in Fig. 15c increased with increasing forge pressure. In particular, all joints fractured from the P-Ti base metal at a forge pressure of 240 MPa or higher. That is, the joint at a friction pressure of 30 MPa, which was made under the following condition, had 100% efficiency and the P-Ti side base metal fracture with no crack at the weld interface: a friction time of 3.0 s or longer and a forge pressure of 270 MPa or higher.

Figure 18 shows the relationship between the forge pressure and joint efficiency of the joints with a friction pressure of 90 MPa which were made at friction times of 0.8 and 2.0 s. The joint efficiency of the joint at a friction time of 0.8 s, which the friction torque reached just after the initial peak, increased with increasing forge pressure, as shown in Fig. 18a. When the joint was made with a forge pressure of 240 MPa or higher, some joints had about 100% joint efficiency. However, the joint efficiency had a scattering, and almost all joints fractured at the weld interface as shown in Fig. 12 although some joints had the P-Ti base metal fracture as shown in Fig. 16. Moreover, the joint efficiency also increased with increasing forge pressure when the joint was made at a friction time of 2.0 s, which the temperature at the periphery portion of the weld interface achieved around 1,150 K (see Fig. 4), as shown in Fig. 18b. Almost all joints also fractured at the weld interface as shown in Fig. 12, although some joints had the P-Ti base metal fracture. That is, it was difficult to reliably obtain the joint with a friction pressure of 90 MPa that had 100% joint efficiency with the P-Ti side base metal fracture. In this connection, the fractured surfaces of the joint with the weld interface fracture did not have the IMC layer, because the weld interface did not have the IMC layer (see Figs. 9 and 10).

To clarify the difference of the joint fractured portion by friction pressure, the cross-section of the joints at various forge pressures were observed. Figures 19 and 20 show the cross-sectional appearances of the weld interface region of the joint with friction pressures of 30 and 90 MPa. In this case, the cross section of the joints with the forge pressure equal to the friction pressure were demonstrated above, i.e. that with a forge pressure of 30 MPa was shown in Fig. 7c, and that of 90 MPa was shown in Fig. 8d, respectively. When the joint was made at a friction pressure of 30 MPa with a friction time of 1.2 s, i.e. the friction torque close to the initial peak as shown in Fig. 1, the weld interface was clear and almost flat at a forge pressure of 30 MPa (see Fig. 7c). In addition, the weld interface did not have a not-joined region, and the LCS side was hardly deformed although the P-Ti side had flash themselves. The LCS side was slightly deformed and a part of it was exhausted as flash from the peripheral portion of the weld interface with increasing forge pressure as shown in Fig. 19a-i. Then, the P-Ti side was slightly deformed to a concave shape, i.e. whole weld interface was not flat (Fig. 19a-ii). Moreover, when the joint was made at a friction time of 3.0 s, the weld interface was also almost flat and the LCS side was hardly deformed at a forge pressure of 30 MPa (see Fig. 7d). The LCS side was deformed with increasing forge pressure and

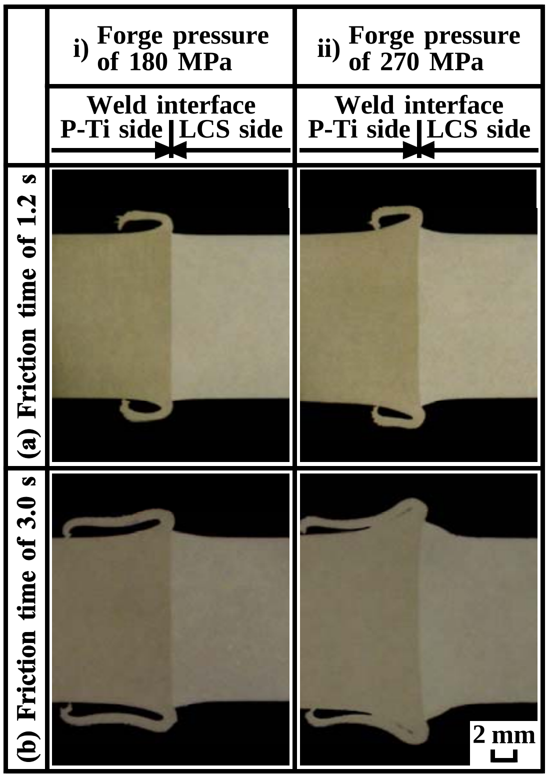

Fig. 19 Cross-sectional appearances of weld interface region of joints at various forge pressures; friction pressure of 30 MPa and friction times of 1.2 and 3.0 s.

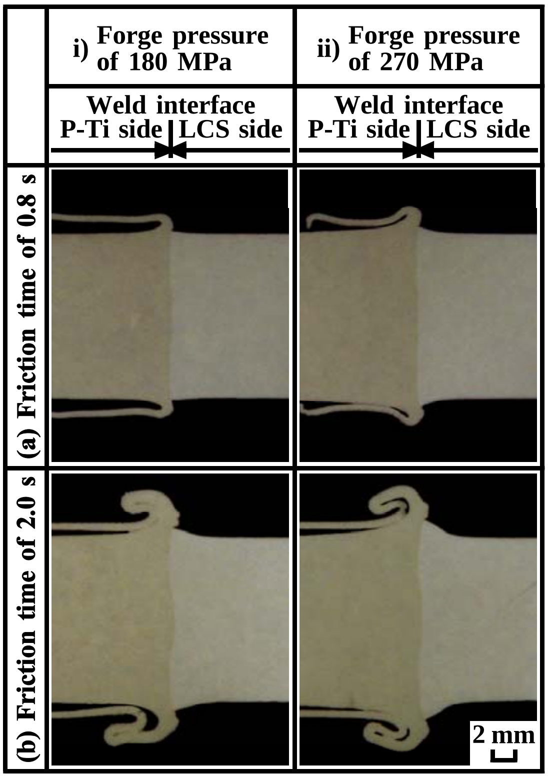

Fig. 20 Cross-sectional appearances of weld interface region of joints at various forge pressures; friction pressure of 90 MPa and friction times of 0.8 and 2.0 s.

whole weld interface was demonstrated as a concave shape from the viewpoint of the P-Ti side as shown in Fig. 19b-i. Then, the LCS side was heavily deformed, that had about 15 mm or over in the length of the radial direction of the joint, i.e. the joint was obtained more LCS flash (Fig. 19b-ii). Furthermore, the joint at a friction time of 8.0 s had also large deformation of the LCS side when it was made with high forge pressure although the quantity of the P-Ti and LCS flashes increased. That is, the P-Ti side had deformation of a concave shape and the joint had generated more LCS flash, when it was made at a friction time of 3.0 s or longer and high forge pressure such as 270 MPa or higher. Hence, the joint with high forge pressure was able to obtain the P-Ti base metal fracture, because the initial oxide film at the weld faying surface of the LCS side was able to estimate as the flash which exhausted from the weld interface during the friction process. Therefore, it is considered that the making joint by high forge pressure is one of a necessary condition for obtaining 100% joint efficiency and the P-Ti side fracture with no crack at the weld interface.

On the other hand, the weld interface was clear and almost flat at a forge pressure of 90 MPa when the joint was made at a friction pressure of 90 MPa with a friction time of 0.8 s (see Fig. 8d). This joint did not have also a not-joined region at the weld interface, and the LCS side was also hardly deformed. When the joint was made at a forge pressure of 180 MPa as shown in Fig. 20a-i, the LCS side was slightly deformed and a part of it was exhausted as flash from the peripheral portion at the weld interface with increasing forge pressure. Therefore, the initial oxide film at the weld faying surface of the LCS side was also able to estimate as the flash which exhausted from the weld interface at this forge pressure. However, the central portion at the weld interface was also slightly demonstrated as a convex shape from the viewpoint of the P-Ti side. This deformation at the weld interface had a reversed direction of the joint with a friction pressure of 30 MPa, i.e. the deformation behaviour of the joint was differed. Then, the flash quantity of the LCS and P-Ti sides increased with increasing forge pressure as shown in Fig. 20a-ii. Furthermore, the deformation behaviour of the joint with a friction time of 2.0 s resembled that of 0.8 s, although the quantity of flashes differed (Fig. 20b). In particular, the length of the radial direction at the LCS side of the joint with a forge pressure of 270 MPa as shown in Fig. 20b-ii were similar to that of a friction pressure of 30 MPa as shown in Fig. 19b-ii. However, the joint with high forge pressure was not able to obtain the P-Ti base metal fracture easily. Hence, another factor seems to be the cause of the weld interface fracture for the joint with a friction pressure of 90 MPa.

4.3 Influence of weld interface temperature for joint strength

As shown in Figs. 19 and 20, it was noteworthy that

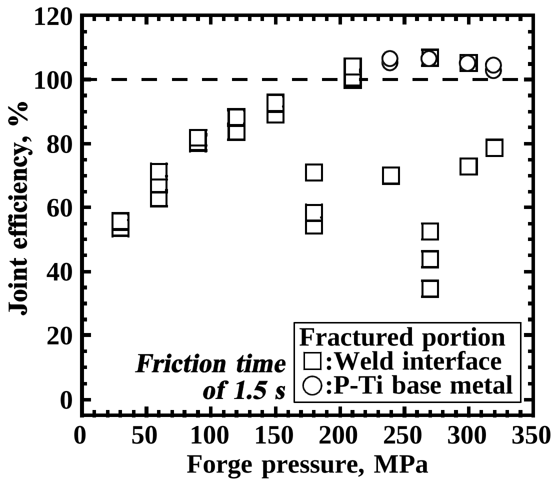

Fig. 21 Relationship between forge pressure and joint efficiency of joint at friction pressure of 30 MPa with friction time of 1.5 s.

the weld interface of the joint with a friction pressure of 90 MPa had a convex shape from the viewpoint of the P-Ti side whereas that of 30 MPa had a concave shape. Incidentally, the temperature of the whole weld interface at a friction pressure of 30 MPa reached to approximately 1,150 K at a friction time of 3.0 s or longer (see Fig. 3). In comparison with this joint, the half radius and centreline portion temperatures of the weld interface at a friction pressure of 90 MPa were not reached to approximately 1,150 K, although that periphery portion was reached to its temperature (see Fig. 4). That is, it was considered that the weldability between P-Ti and LCS was poor at the temperature of the weld interface below 1,150 K. Therefore, we investigated the effect of forge pressure on the tensile strength of the joint at a friction pressure of 30 MPa with a friction time of 1.5 s, because the temperature at the adjacent region of whole weld interface was approximately 1,000 K at this friction time as shown in Fig. 3. In this connection, this temperature was close to the central portion of the weld interface of the joint at a friction pressure of 90 MPa with a friction time of 2.0 s (see Figs. 3 and 4). If the weldability between P-Ti and LCS was not poor at this temperature (approximately 1,000 K) on the weld interface, the joint should be easily obtained 100% efficiency and the P-Ti base metal fracture. Figure 21 shows the relationship between the forge pressure and joint efficiency of the joints under a friction pressure of 30 MPa with a friction time of 1.5 s. The joint efficiency increased with increasing forge pressure, and then some joints achieved 100% joint efficiency with the P-Ti base metal fracture as shown in Fig. 15 when it was made with a forge pressure of 270 MPa or higher. However, the joint efficiency had a scattering, and many joints fractured at the weld interface as shown in Fig. 12. That is, the joint, which had 100% joint efficiency with the P-Ti side base metal fracture, was not easily obtained at a friction time of 1.5 s. Hence, the weld interface of the joint seems to be necessary to achieve high temperature of around 1,150 K for obtaining the joint with 100% joint efficiency and the P-Ti side base metal fracture. In case of diffusion welding, the joint with a bonding temperature below 1,123 K was not obtained 100% joint efficiency although that with a bonding temperature of around 1,173 K was easily obtained its efficiency [31,32]. Therefore, it is considered that the achievement of the temperature at whole weld interface of around 1,173 K is also necessary condition for obtaining 100% joint efficiency and the P-Ti side fracture with no crack at the weld interface.

According to the result described above, the difference of the joint fractured portion was due to the large deformation of the LCS side and the shape of the weld interface which was depended on the deformation of the P-Ti and LCS sides. Moreover, those had difference with the maximum temperature at the weld interface which was depended on the applied friction pressure. It is considered that the further investigation must elucidate the detailed joint properties such as hardness at the adjacent region of the weld interface or the fractured surface analysis by X-ray diffraction technique. However, to obtain 100% joint efficiency and the P-Ti base metal fracture with no crack at the weld interface, the joint should be made with high forge pressure, low friction pressure, and with opportune friction time at which the temperature at whole weld interface reached around 1,150 K.

5. Conclusions

This report described the effect of friction welding condition on joining phenomena and tensile strength of friction welded joint between pure titanium (P-Ti) and low carbon steel (LCS). The following conclusions are provided.

(1) The adjacent region of the weld interface at the P-Ti side had large deformation and intensely upset when the joint had sparkle in spite of applied friction pressure, although that of the LCS side was hardly upset. Also, the entire weld interface at the LCS side had transferred P-Ti when the friction torque reached the initial peak.
(2) The temperature of the whole weld interface at a friction pressure of 30 MPa reached to 1,150 K or over at a friction time of 3.0 s or longer. On the other hand, the half radius and centreline portion temperatures of the weld interface at a friction pressure of 90 MPa was not reached to 1,150 K, although the periphery portion of that was reached to its temperature.
(3) The central portion of the weld interface at a friction pressure of 90 MPa was deformed to a convex shape from the viewpoint of the P-Ti side, although that of 30 MPa remained almost flat after when the friction torque reached the initial peak. The fact that the weld interface shape had dissimilarity was due to the difference of the maximum temperature at the weld interface with applied friction pressure.

(4) An IMC layer was not observed at the weld interface of the joint at applied friction pressures of 30 and 90 MPa, which was based on the SEM observation level.
(5) The joining phenomena during the friction process at a friction pressure of 30 MPa were similar to that of 90 MPa, in spite of the difference of both the maximum temperature at the weld interface and the weld interface deformation.
(6) The joint, which was made with a forge pressure of applied identical friction pressure, did not achieve 100% joint efficiency, although it increased with increasing friction pressure.
(7) When the joint was made with a friction pressure of 30 MPa, the joint efficiency increased with increasing forge pressure. Then, when the joint was made with a friction time of 3.0 s or longer, and a forge pressure of 270 MPa or higher, it achieved 100% joint efficiency and the P-Ti base metal fracture with no crack at the weld interface.
(8) Many joints, which was made with a friction pressure of 30 MPa, friction times of 1.2 and 1.5 s, and high forge pressure, was fractured at the weld interface, although those achieved 100% joint efficiency.
(9) When the joint was made with a friction pressure of 90 MPa, the joint efficiency also increased with increasing forge pressure. However, many joints fractured at the weld interface, although those achieved 100% joint efficiency.
(10) The difference of the fractured portion of the joint in both applied friction pressures was due to the difference between the maximum temperature at the weld interface during the friction process and the deformation amount of the LCS side caused by applied forge pressure.

In conclusion, to obtain 100% joint efficiency with the P-Ti base metal fracture with no crack at the weld interface, the joint should be made with high forge pressure, low friction pressure, and with opportune friction time at which the temperature at whole weld interface reached around 1,150 K.

Acknowledgements

A part of this research was partially supported by the Ministry of Education, Culture Sports, Science and Technology, Grant-in-Aid for Young Scientists (B), 20760496, 2010-2011. We wish to thank the staff members of the Machine and Workshop Engineering at the Graduate School of Engineering, University of Hyogo. We also wish to thank the alumnus Mr Tetsuya Tsujimoto for his devoted contributions to this research project. Also, we wish to thank Mr Hideaki Tohkuni in Kitami Institute of Technology for his kindly and aggressive assisting to this study.

References

[1] American Welding Society. Welding Handbook. 7th Edition. Vol. 4. Miami. FL: American Welding Society; 1982. p. 537-8.
[2] Kotaki H. Welding Technique of Titanium. Tokyo: Nikkan Kogyo Shinbunsha Publishers; 2000. p. 82 (in Japanese).
[3] Hasui A, Kira Y. Friction welding of Titanium and Plain Carbon Steel. Q J Jpn Weld Soc 1983; 1(3): 366-71 (in Japanese).
[4] Shinoda T, Takegami H. Friction Welding of Titanium and Carbon Steel. Proc Symp Weld Mech Des. Japan Welding Society 1999; 247-54 (in Japanese).
[5] Meshram SD, Mohandas T, Reddy GM. Friction welding of dissimilar pure metals. J Mater Process Technol 2007; 184: 330-37.
[6] Lee WB, Jung SB. Effect of Microstructure on Mechanical Properties of Friction-Welded Joints between Ti and AISI 321 Stainless Steel. Mater Trans 2004; 45(9): 2805-11.
[7] Dey HC, Ashfaq M, Bhaduri AK, Rao KP. Joining of titanium to 304L stainless steel by friction welding. J Mater Process Technol 2009; 209(18/19): 5862-70.
[8] Akbarimousavi SAA, GohariKia M. Investigations on the mechanical properties and microstructure of dissimilar cp-titanium and AISI 316L austenitic stainless steel continuous friction welds. Mater Des 2011; 32(5): 3066-75.
[9] Fuji A, North TH, Ameyama A, Futamata M. Improving tensile strength and bend ductility of titanium/AISI 304L stainless steel friction welds. Mater Sci Technol 1992; 8(3): 219-35.
[10] Futamata M, Fuji A. Study of Friction Welding of Titanium and SUS 304L Austenitic Stainless Steel. Q J Jpn Weld Soc 1989; 7(4): 432-8 (in Japanese).
[11] Kim YC, Fuji A, North TH. Improving Bend Ductility in Titanium/AISI304L Stainless Steel Friction Welds. J High Temp Soc Jpn 1996; 22(2): 94-9 (in Japanese).
[12] Ochi H, Ogawa K, Kaga S, Ohike H, Suga Y. Friction welding of titanium and SUS304 stainless steel. J Jpn Inst Light Met 1993; 43(7): 365-71 (in Japanese).
[13] Wang KK. Friction Welding. Welding Research Council Bulletins 1975; 204: 1-21.
[14] Kimura M, Mioh H, Kusaka M, Seo K, Fuji A. Observation of Joining Phenomena in First Phase of Friction Welding. Q J Jpn Weld Soc 2002; 20(3): 425-31 (in Japanese).
[15] Kimura M, Kusaka M, Seo K, Fuji A. Effect of Various Conditions on Friction Torque in the First Phase of Friction Welding. Q J Jpn Weld Soc 2002; 20(3): 432-38 (in Japanese).
[16] Kimura M, Kusaka M, Seo K, Fuji A. Relationship between the Friction Time, Friction Torque, and Joint Properties of Friction Welding for the Low Heat Input Friction Welding Method. Q J Jpn Weld Soc 2002; 20(4): 559-65 (in Japanese).
[17] Kimura M, Ohtsuka Y, An GB, Kusaka M, Seo K, Fuji A. Effect of Friction Speed on Initial Seizure

Portion on Welded Interface. Q J Jpn Weld Soc 2003; 21(4): 615-22 (in Japanese).
[18] Kimura M, An GB, Kusaka M, Seo K, Fuji A. An Experimental Study of Seizure Phenomena at Welded Interface of Steel Friction Weld. Q J Jpn Weld Soc 2005; 23(3): 460-8 (in Japanese).
[19] Kimura M, Kusaka M, Seo K, Fuji A. Observation of Joining Phenomena in Friction Stage and Improving Friction Welding Method. JSME Int J Series A 2003; 46(3): 384-90.
[20] Kimura M, Kusaka M, Seo K, Fuji A. Joining phenomena during friction stage of A7075-T6 aluminium alloy friction weld. Sci Technol Weld Joining 2005; 10(3): 378-83.
[21] Kimura M, Kusaka M, Seo K, Fuji A. Relationship between Joining Phenomena and Yield Strength of Substrates of Dissimilar Friction Welding. Q J Jpn Weld Soc 2003; 21(3): 481-8 (in Japanese).
[22] Kimura M, Ishii H, Kusaka M, Kaizu K, Fuji A. Joining phenomena and joint strength of friction welded joint between pure aluminium and low carbon steel. Sci Technol Weld Joining 2009; 14(5): 388-95.
[23] Kimura M, Ishii H, Kusaka M, Kaizu K, Fuji A. Joining phenomena and joint strength of friction welded joint between aluminium-magnesium alloy (AA5052) and low carbon steel. Sci Technol Weld Joining 2009; 14(7): 655-61.
[24] Kimura M, Kusaka M, Kaizu K, Fuji A. Effect of Friction Welding Condition on Joining Phenomena and Tensile Strength of Friction Welded joint between Pure Copper and Low Carbon Steel. J Solid Mech Mater Eng 2009; 3(2): 187-98.
[25] Kimura M, Kasuya K, Kusaka M, Kaizu K, Fuji A. Effect of friction welding condition on joining phenomena and joint strength of friction welded joint between brass and low carbon steel. Sci Technol Weld Joining 2009; 14(5): 404-12.
[26] Kimura M, Saitoh Y, Kusaka M, Kaizu K, Fuji A. Effect of friction pressure on joining phenomena of friction welds between pure titanium and pure copper. Sci Technol Weld Joining 2011; 16(5): 392-8.
[27] Kimura M, Inoue H, Kusaka M, Kaizu K, Fuji A. Analysis method of friction torque and weld interface temperature during friction process of steel friction welding. J Solid Mech Mater Eng 2010; 4(3): 401-13.
[28] Kimura M, Ichihara A, Kusaka M, Kaizu K. Joint properties and their improvement of AISI 310S austenitic stainless steel thin walled circular pipe friction welded joint. Mater Des 2012; 38: 38-46.
[29] American Welding Society. Welding Handbook. 7th Edition. Vol. 4. Miami. FL: American Welding Society; 1982. p. 434-73.
[30] The Japan Society for Technology of Plasticity. Fundamentals of Titanium and Its Working. Tokyo: Corona Publising; 2008. p. 179-94 (in Japanese).
[31] Momono T, Enjo T, Ikeuchi K. Effects of Carbon Content on the Diffusion Bonding of Iron and Steel to Titanium. ISIJ Int 1990; 30(11): 978-84.
[32] Kanai S, Seto S, Ito M. The Effects of Reaction Phases on the Strength Properties of Diffusion Bonds Formed between Bearing Steel SUJ2 and Ti-6Al-4V Alloy. Q J Jpn Weld Soc 2005; 23(3): 484-90 (in Japanese).